

BB  
MICHIGAN STATE  
UNIVERSITY

National Superconducting Cyclotron Laboratory

**BETA DECAY STUDIES OF NUCLEI NEAR  $^{32}\text{Mg}$ : INVESTIGATING  
THE  $\nu(f_{7/2})-(d_{3/2})$  INVERSION AT THE  $N = 20$  SHELL CLOSURE**

**A.C. MORTON, P.F. MANTICA, B.A. BROWN, A.D. DAVIES,  
D.E. GROH, P.T. HOSMER, S.N. LIDDICK, J.I. PRISCIANDARO,  
H. SCHATZ, M. STEINER, and A. STOLZ**

  
CERN LIBRARIES, GENEVA



CM-P00040542

  
NSCL

MSUCL-1240

SEPTEMBER 2002

# Beta decay studies of nuclei near $^{32}\text{Mg}$ : Investigating the $\nu(f_{7/2})-(d_{3/2})$ inversion at the $N = 20$ shell closure

A.C. Morton<sup>a</sup>, P.F. Mantica<sup>a,b</sup>, B.A. Brown<sup>a,c</sup>, A.D. Davies<sup>a,c</sup>,  
D.E. Groh<sup>a,b</sup>, P.T. Hosmer<sup>a,c</sup>, S.N. Liddick<sup>a,b</sup>,  
J.I. Prisciandaro<sup>a,b</sup>, H. Schatz<sup>a,c</sup>, M. Steiner<sup>a</sup>, and A. Stolz<sup>a</sup>

<sup>a</sup>*National Superconducting Cyclotron Laboratory, Michigan State University, East Lansing, MI 48824 USA*

<sup>b</sup>*Department of Chemistry, Michigan State University, East Lansing, MI 48824 USA*

<sup>c</sup>*Department of Physics and Astronomy, Michigan State University, East Lansing, MI 48824 USA*

---

## Abstract

$^{32}\text{Mg}$  lies within a region of deformed nuclei commonly referred to as the “island of inversion”. The  $\beta$  decay of  $^{33}\text{Al}$  and  $^{33}\text{Mg}$  has been studied to learn about nuclear structure near  $^{32}\text{Mg}$ . Decay curves and precise half-life measurements are presented for both species. Gamma-ray spectra from correlated  $^{33}\text{Al}$  decay events are also presented. The  $\beta$ -decay properties of  $^{33}\text{Al}$  are shown to be well-described by an *sd* shell model calculation, suggesting that the ground state of  $^{33}\text{Al}$  lies primarily outside the island of inversion.

---

The region near  $^{32}\text{Mg}$  is interesting from a nuclear structure standpoint. Mass measurements of  $^{31}\text{Na}$  and  $^{32}\text{Na}$  by Thibault *et al.* [1] produced the first evidence of nuclear deformation in neutron-rich nuclei near the  $N = 20$  shell closure. This deformation has been attributed to an inversion of the order in which the  $\nu(f_{7/2})$  and  $\nu(d_{3/2})$  orbitals are filled [2–4]. In its ground state,  $^{32}_{12}\text{Mg}_{20}$  has been shown [5–7] to lie within this region of deformation, the so-called “island of inversion” [3]. The ground state of  $^{34}_{14}\text{Si}_{20}$ , with two additional protons, is believed to be spherical [8–10]. The structure of  $^{33}_{13}\text{Al}_{20}$  is unknown.

Beta decay properties of nuclei far from the valley of stability can serve as probes of nuclear structure. In the current work, we have studied the  $\beta$  decay of  $^{33}\text{Al}$  and  $^{33}\text{Mg}$  to learn about structure near  $^{32}\text{Mg}$ . Precise half-lives have been deduced for both species. A  $\beta$ -delayed  $\gamma$ -ray spectrum for the decay of

$^{33}\text{Al}$  has also been obtained and absolute  $\gamma$ -ray intensities determined. These results are compared with those of shell model calculations.

$^{33}\text{Mg}$ ,  $^{33}\text{Al}$  and other neutron-rich species were produced by projectile fragmentation of 140 MeV/nucleon  $^{40}\text{Ar}^{18+}$  in a 1455 mg/cm<sup>2</sup> beryllium target using the new Coupled Cyclotron Facility at the National Superconducting Cyclotron Laboratory at Michigan State University. Nuclides of interest were separated from other reaction products using the A1900 fragment analyzer and delivered to the experimental end station. A 4 cm  $\times$  4 cm double-sided silicon strip detector (DSSD) was used as both a fragment implantation target and a monitor of  $\beta$ -decay activity [11]. This detector is highly segmented with 40 one-millimeter-wide strips in each direction and is 985  $\mu\text{m}$  thick, providing sufficient depth of silicon for the observation of high-energy  $\beta$  decays. The energy resolution of the DSSD was measured using  $\alpha$  particles from a  $^{228}\text{Th}$  source; that of individual strips was found to be better than 80 keV FWHM at 8.78 MeV. Aluminum degraders were used to reduce the energy of the incoming fragments so that they would be stopped in the front 200  $\mu\text{m}$  of the DSSD. Three 5 cm  $\times$  5 cm silicon PIN diodes were placed near the DSSD to differentiate implantation and decay events. The first of these was 488  $\mu\text{m}$  thick and was placed 22 mm upstream of the DSSD. The other two, 309 and 303  $\mu\text{m}$  thick, were placed 23 and 27 mm downstream of the DSSD, respectively. An additional 5 cm  $\times$  5 cm  $\times$  500  $\mu\text{m}$  PIN diode was located  $\sim$ 1 m upstream of the DSSD array to provide energy loss and time-of-flight information for particle identification purposes. A parallel-plate avalanche counter (PPAC) located just upstream of this PIN provided redundant position information. Finally, two high-purity germanium (HPGe)  $\gamma$ -ray counters were installed in close geometry in order to study  $\beta\gamma$  coincidences. One, with 80% efficiency relative to a 3"  $\times$  3" NaI detector, was placed on the beam axis 8.9 cm downstream of the DSSD. The second had an efficiency of 120% and was placed 14.0 cm from the center of the DSSD. This HPGe detector was located 45° off the beam axis on the upstream side of the DSSD. The total peak  $\gamma$  ray detection efficiency was 0.76% at  $E_\gamma = 1.0$  MeV. The energy resolution of the 80% HPGe detector was measured to be 3.5 keV FWHM at 1.33 MeV; that of the 120% detector was measured to be 4.8 keV.

Dual-output preamplifiers with separate low- and high-gain outputs were used with the DSSD in order to obtain energy information for high-energy ( $\sim$ 1 GeV) implantation events and low-energy ( $\sim$ 1 MeV)  $\beta$  decays, respectively. Data acquisition was triggered solely on high-gain signals. Events were identified as fragment implantations if low-gain signals were observed in both front and back strips in coincidence with signals in both upstream PIN diodes. Decay events were identified by the observation of high-gain signals in both front and back strips in anticoincidence with signals in the furthest upstream PIN. Implant and decay events were directly correlated on a pixel-by-pixel basis within the DSSD. Each event was time-stamped with 30.5  $\mu\text{s}$  resolution; de-

cay times were determined by subtracting the time at which a fragment was implanted from that of its subsequent  $\beta$  decay.

The direct correlation of implants and decays requires that a given implanted fragment decay before the next fragment is implanted within that pixel. In order to maximize the time between implants within a specific pixel, the incoming fragment beam was deliberately defocused in both the  $x$ - and  $y$ -directions to illuminate as many pixels as possible. The fragment distribution was roughly Gaussian in both  $x$  and  $y$  with a full width at half maximum of 20 strips in each direction. Typical total implantation rates were 20–50 s<sup>-1</sup> so that the average time between implants within a given pixel was 30–80 s (*i.e.* much longer than the decay times of the nuclei of interest). When two implantations were recorded in one pixel before the observation of a decay event, both were rejected if the time between the implants was less than the greater of five times the half-life of the initial implanted nucleus (or, in the case of <sup>33</sup>Al, that of the <sup>33</sup>Si daughter) or 1 s. Correlated <sup>33</sup>Al and <sup>33</sup>Mg events with decay times longer than 1 or 5 s, respectively, were also rejected. Correlation efficiencies of 14 and 38% were observed for <sup>33</sup>Al and <sup>33</sup>Mg, respectively.

Data were taken in two consecutive running periods. A 330 mg/cm<sup>2</sup> Al wedge was placed at the dispersive plane of the A1900 fragment analyzer to reduce background components in the secondary beams. During the first period, the magnetic rigidity of the A1900's first two dipole elements,  $B\rho_1$ , was set to 3.5300 T·m while that of the second two dipoles,  $B\rho_2$ , was set to 3.2958 T·m. This optimized the yield of <sup>33</sup>Al. Over two days,  $1.95 \times 10^6$  fragments were implanted. <sup>33</sup>Al ions accounted for 62.1% of these fragment implants. The main beam impurities were <sup>34</sup>Si and <sup>35</sup>Si, accounting for 33.9% and 2.6% of implants, respectively. In the second period,  $B\rho_1$  was set to 3.9444 T·m and  $B\rho_2$  to 3.7462 T·m to optimize the yield of <sup>33</sup>Mg. Beam contaminants included <sup>31</sup>Na, <sup>34,35</sup>Al, and <sup>36</sup>Si. In 14 hours  $3.39 \times 10^5$  fragments were implanted. Of these, 12.9% were <sup>33</sup>Mg ions, 31.1% were <sup>34</sup>Al ions, and 50.9% were <sup>35</sup>Al ions. By defining appropriate gates in the energy loss versus time-of-flight spectra from correlated implant events,  $\beta$ -decay lifetime curves were obtained for both <sup>33</sup>Al and <sup>33</sup>Mg. Beta-delayed  $\gamma$ -ray spectra were also obtained for the decay of <sup>33</sup>Al.

The <sup>33</sup>Al decay curve is shown in Figure 1. To properly account for both the <sup>33</sup>Al parent activity and the <sup>33</sup>Si daughter, the decay curve was fitted with a two-component function with a long-lived exponential background where the components of the fit were calculated from Bateman equations [12]. Based on the observation of  $1.7 \times 10^5$   $\beta$  decays correlated with <sup>33</sup>Al implant events, the  $\beta$ -decay half-life,  $T_{1/2}^\beta$ , was deduced to be  $41.7 \pm 0.2$  ms. No prior measurement of the half-life has been published.

Correlated  $\gamma$ -ray spectra are shown in Figure 2. Figures 2a) and 2b) include

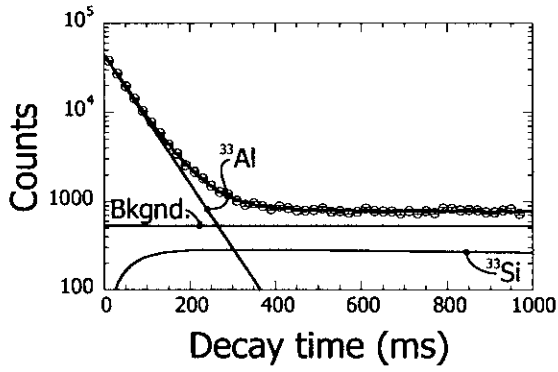


Fig. 1.  $^{33}\text{Al}$  decay curve, showing fit components.

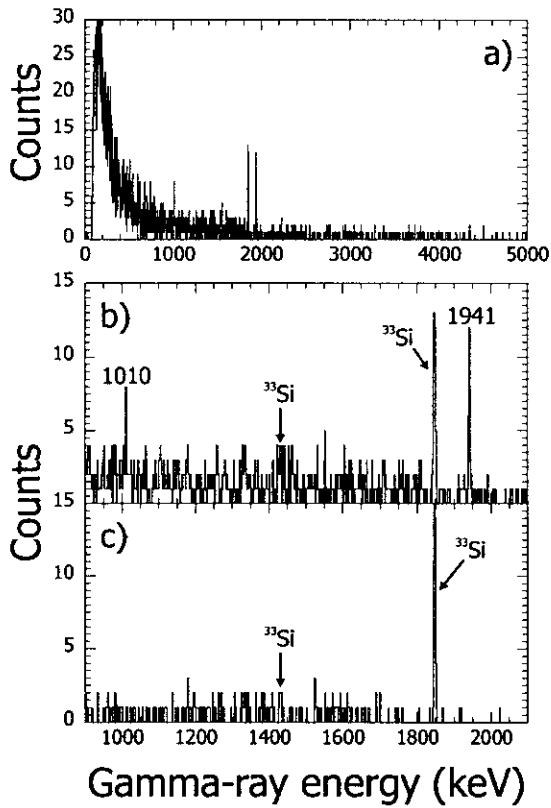


Fig. 2. Gamma-ray spectra from the decay of  $^{33}\text{Al}$ : a) decay time,  $t_d$ , less than 0.5 s; b)  $t_d < 0.5$  s; c)  $0.5 \text{ s} \leq t_d < 1.0$  s.

events with decay time,  $t_d$ , less than 0.5 s and contain all of the observed  $^{33}\text{Al}$  decay  $\gamma$  rays. Figure 2c) includes events with  $0.5 \text{ s} \leq t_d < 1.0$  s and is dominated by  $\gamma$  rays from the decay of the daughter nucleus,  $^{33}\text{Si}$  [13]. Peaks in the  $^{33}\text{Al}$   $\beta$ -delayed  $\gamma$ -ray spectrum are listed in Table 1. This is the first reported observation of delayed  $\gamma$  rays from  $^{33}\text{Al}$   $\beta$  decay. With the exception of that at  $4341 \pm 11$  keV, these peaks were fitted with Gaussian distributions over linear backgrounds using the spectrum analysis package DAMM [14].

Table 1  
Transitions in the  $^{33}\text{Al}$   $\beta$ -delayed  $\gamma$  ray spectrum.

| $E_\gamma$ (keV) | $I_{\text{abs}}(\%)$ | Identification   |
|------------------|----------------------|--|
| $1010.2 \pm 0.5$ | $1.0 \pm 0.3$        | $\beta$ -delayed; decay of first $1/2^+$ state in $^{33}\text{Si}$ |
| $1431.5 \pm 0.6$ | N/A                  | $^{33}\text{Si}$ decay [13]  |
| $1847.0 \pm 0.4$ | N/A                  | $^{33}\text{Si}$ decay [13]  |
| $1940.5 \pm 0.2$ | $2.5 \pm 0.3$        | $\beta n$ -delayed; decay of first $2^+$ state in $^{32}\text{Si}$ |
| $4341 \pm 11$    | $1.3_{-0.6}^{+0.7}$  | $\beta$ -delayed; decay of first $5/2^+$ state in $^{33}\text{Si}$ |

The  $^{33}\text{Al}$  decay spectrum contains a peak at  $1940.5 \pm 0.2$  keV with an absolute intensity of  $2.5 \pm 0.3\%$ . This is identified as the decay of the first excited  $2^+$  state in  $^{32}\text{Si}$  [15] populated by  $\beta$ -delayed neutron emission from  $^{33}\text{Al}$ , and represents the first observation of a  $\beta n$ -delayed  $\gamma$  ray from the decay of  $^{33}\text{Al}$ . Reeder *et al.* claim a total  $\beta$ -delayed neutron probability,  $P_n$ , for  $^{33}\text{Al}$  of  $8.5 \pm 0.7\%$  [16]. The present result does not contradict this earlier, unpublished, measurement as the current experiment is not sensitive to all  $\beta n$  decay channels.

The peak at  $1010.2 \pm 0.5$  keV with an absolute intensity of  $1.0 \pm 0.3\%$  is identified as the decay of the first excited state in  $^{33}\text{Si}$ . This state has been shown to have  $J^\pi = 1/2^+$  [17,18] so that  $\beta$  feeding from the  $5/2^+$   $^{33}\text{Al}$  ground state would be second-forbidden. The population of this state is instead attributed to the deexcitation of higher-energy states populated in the  $\beta$  decay of  $^{33}\text{Al}$ .

A sharp cutoff in the  $\gamma$ -ray spectrum is observed near 4350 keV, similar to that reported by Pritychenko *et al.* [18]. This is identified as the deexcitation of the first excited  $5/2^+$  state in  $^{33}\text{Si}$ . The FWHM of a peak at this energy was estimated to be 12 keV, based on measurements made at lower energies with calibration sources. The intensity of the transition was determined by integrating over a 30 keV range of  $\gamma$ -ray energies centered on an apparent excess of counts above background near 4340 keV. The observed  $\gamma$ -ray energy of  $4341 \pm 11$  keV is consistent with that reported by Enders *et al.* ( $4290 \pm 140$  keV [17]) and with the previously-measured level energy of  $4320 \pm 30$  keV [8]. An absolute intensity of  $1.3_{-0.6}^{+0.7}\%$  is observed.

The strongest observed transition associated with the decay of  $^{33}\text{Al}$  has an absolute intensity of less than 3%, while the total intensity of the observed decays from  $^{33}\text{Al}$  ( $4.8 \pm 0.7\%$ ) is less than that of the  $1847.0 \pm 0.4$  keV  $\gamma$  ray from the decay of the  $^{33}\text{Si}$  daughter ( $5.1 \pm 0.5\%$ ). This indicates that  $^{33}\text{Al}$  decays primarily to the ground state of  $^{33}\text{Si}$ . The branching ratio for this decay can be estimated by taking the transitions at  $1010.2 \pm 0.5$  and  $4341 \pm 11$  keV to be independent of one another and including the  $P_n$  of Reeder *et al.*. After considering the error due to the possibility of further, unobserved,

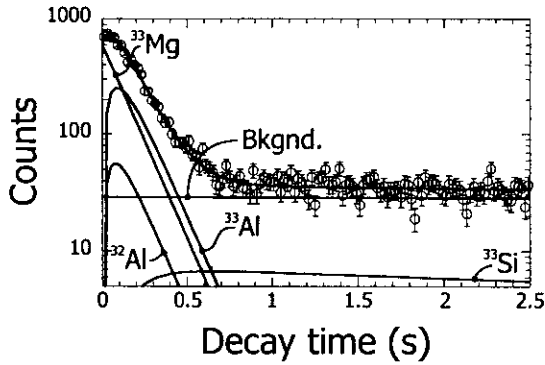


Fig. 3.  $^{33}\text{Mg}$  decay curve, showing fit components.

weak transitions, we adopt a value of  $89^{+10}_{-3}\%$  for the previously-unmeasured branching ratio for the ground-state  $\beta$  decay of  $^{33}\text{Al}$ .

The  $^{33}\text{Mg}$  decay curve is shown in Figure 3. As the  $^{33}\text{Mg}$  parent activity; the  $\beta$ -decay daughter,  $^{33}\text{Al}$ ; the  $\beta$ -decay granddaughter,  $^{33}\text{Si}$ ; and the  $\beta n$  daughter,  $^{32}\text{Al}$ ; were all expected to contribute to the curve, it was fitted with a four-component function with an additional exponential background. The contribution of each nucleus was again determined using Bateman equations, with the  $\beta$ -delayed neutron branch taken to be 17% [19]. On the basis of  $1.6 \times 10^4$  observed  $^{33}\text{Mg}$ -correlated decay events  $T_{1/2}^\beta$  was determined to be  $90.5 \pm 1.6$  ms, in excellent agreement with, and an order of magnitude more precise than, the previously-reported value of  $90 \pm 20$  ms [19].

Shell-model results for the  $\beta$  decay of  $^{33}\text{Al}$  and the subsequent  $\gamma$  decay in  $^{33}\text{Si}$  were obtained in the full  $sd$  shell basis with the USD Hamiltonian and the effective Gamow-Teller and electromagnetic operators summarized in [20]. The  $\beta$ -decay properties for these neutron-rich  $sd$  shell nuclei were predicted in 1983 using the same USD Hamiltonian [21]. The present  $\beta$ -decay calculations differ from those reported earlier in the use of a more precise effective Gamow-Teller operator and the inclusion of updated experimental  $\beta$ -decay Q values; in 1983, that of  $^{32}\text{Mg}$   $\beta$  decay was not known. For the  $N = 20$  nuclei on the edge of the island of inversion, the  $\beta$ -decay half-lives from the present calculation are 3100, 34.8 and 26 ms for  $^{34}\text{Si}$ ,  $^{33}\text{Al}$  and  $^{32}\text{Mg}$ , respectively, compared to experimental values of  $2800 \pm 200$  [21] for  $^{34}\text{Si}$ ,  $41.7 \pm 0.2$  from the present experiment for  $^{33}\text{Al}$ , and  $120 \pm 20$  [19] for  $^{32}\text{Mg}$ . From the half-life information alone,  $^{32}\text{Mg}$  is clearly inconsistent with an  $sd$  shell structure and is expected to lie within the island of inversion. Previous work has shown this to be the case [5–7].

A more exacting test of the structure of the  $^{33}\text{Al}$  ground state is provided by a detailed comparison of the experimental and theoretical  $\beta$ -decay branching ratios given in Table 2 and  $\gamma$ -ray intensities given in Table 3.  $^{33}\text{Al}$  is observed to decay to the ground state of  $^{33}\text{Si}$  with a branching ratio of  $89^{+10}_{-3}\%$ ; this

Table 2  
Results of an *sd* shell model calculation for  $^{33}\text{Al}$   $\beta$  decay.

| Input $J^\pi, T$ ( $^{33}\text{Al}$ g.s.)            | 5/2 <sup>+</sup> , 7/2 |                                     |
|--|------------------------|-------------------------------------|
| Experimental $Q_\beta$                               | 11.990 MeV             |                                     |
|  | Calculated             | Observed                            |
| $T_{1/2}^\beta$ (ms)                                 | 34.8                   | 41.7 ± 0.2                          |
| $\beta$ -decay BR to states in $^{33}\text{Si}$ (%): |                        |                                     |
| Neutron-bound daughter states:                       |                        |                                     |
| 0.000 MeV (3/2 <sup>+</sup> )                        | 87.7                   | 89 <sup>+1</sup> <sub>-3</sub>      |
| 3.985 (7/2 <sup>+</sup> )                            | 0.2                    |                                     |
| 4.378 (5/2 <sup>+</sup> )                            | 1.8                    | 1.3 <sup>+0.7</sup> <sub>-0.6</sub> |
| 4.421 (3/2 <sup>+</sup> )                            | 3.1                    |                                     |
| 4.693 (3/2 <sup>+</sup> )                            | 1.1                    |                                     |
| Neutron-unbound daughter states:                     |                        |                                     |
| All 3/2 <sup>+</sup>                                 | 1.3                    |                                     |
| All 5/2 <sup>+</sup>                                 | 3.3                    |                                     |
| All 7/2 <sup>+</sup>                                 | 1.6                    | ≤ 2.5                               |
| Total  | 6.2                    | 8.5 ± 0.7[16]                       |

agrees with the calculated ground state branch of 87.7%. The  $\gamma$  decay of the first excited 2<sup>+</sup> state in  $^{32}\text{Si}$  populated by  $\beta n$  decay from  $^{33}\text{Al}$  is observed with an intensity of  $2.5 \pm 0.3\%$ . As the current experiment is not sensitive to all modes of neutron decay, this intensity provides a lower limit on  $P_n$ . Furthermore, the branching ratio for  $\beta$  decay to 7/2<sup>+</sup> states above the neutron decay threshold must be less than 2.5%, as these states cannot decay directly to the 0<sup>+</sup> ground state of  $^{32}\text{Si}$ . In comparison, the total  $\beta$ -decay branching ratio to neutron-unbound states in  $^{33}\text{Si}$  is calculated to be 6.2%, with a 1.6% branch to 7/2<sup>+</sup> states. The absolute intensity of the decay of the first excited state in  $^{33}\text{Si}$ , with  $J = 1/2$ , is observed to be  $1.0 \pm 0.3\%$ . This is identified with the calculated  $J = 1/2$  state at 0.848 MeV predicted to decay with an absolute intensity of 2.1%. Finally, the first 5/2<sup>+</sup> state in  $^{33}\text{Si}$  is observed to decay to the ground state with an absolute intensity of  $1.3^{+0.7}_{-0.6}\%$ , consistent with the predicted intensity for this transition of 1.8%. Considering the half-life and the branching ratios for both  $\beta$  and  $\beta n$  decay, the observed decay of  $^{33}\text{Al}$  is well-described by the *sd* shell model calculation, suggesting that  $^{33}\text{Al}$ , in its ground state, lies primarily outside the island of inversion.

An additional shell model calculation has been carried out for the  $\beta$  decay of



Table 3

Gamma-ray intensities for the decay of states in  $^{33}\text{Si}$  populated in the  $\beta$  decay of  $^{33}\text{Al}$ .

| Calculated |             |       |             |                  |                      | Observed         |                      |
|------------|-------------|-------|-------------|------------------|----------------------|------------------|----------------------|
| $J_i$      | $E_i$ (MeV) | $J_f$ | $E_f$ (MeV) | $E_\gamma$ (keV) | $I_{\text{abs}}(\%)$ | $E_\gamma$ (keV) | $I_{\text{abs}}(\%)$ |
| 3/2        | 4.693       | 3/2   | 0.000       | 4693             | 0.2                  |                  |                      |
|            |             | 1/2   | 0.848       | 3845             | 0.9                  |                  |                      |
|            |             | 7/2   | 3.985       | 708              | 0.0                  |                  |                      |
|            |             | 5/2   | 4.378       | 315              | 0.0                  |                  |                      |
|            |             | 3/2   | 4.421       | 272              | 0.0                  |                  |                      |
| 3/2        | 4.421       | 3/2   | 0.000       | 4421             | 1.9                  |                  |                      |
|            |             | 1/2   | 0.848       | 3573             | 1.2                  |                  |                      |
|            |             | 7/2   | 3.985       | 436              | 0.0                  |                  |                      |
|            |             | 5/2   | 4.378       | 43               | 0.0                  |                  |                      |
| 5/2        | 4.378       | 3/2   | 0.000       | 4378             | 1.7                  | 4341 $\pm$ 11    | 1.3 $^{+0.7}_{-0.6}$ |
|            |             | 1/2   | 0.848       | 3530             | 0.0                  |                  |                      |
|            |             | 7/2   | 3.985       | 393              | 0.0                  |                  |                      |
| 7/2        | 3.985       | 3/2   | 0.000       | 3985             | 0.2                  |                  |                      |
| 1/2        | 0.848       | 3/2   | 0.000       | 848              | 2.1                  | 1010.2 $\pm$ 0.5 | 1.0 $\pm$ 0.3        |

$^{33}\text{Mg}$ . Because of the presence of a neutron in the  $pf$  shell, it is more complex than the  $sd$  shell model calculation used to describe the decay of  $^{33}\text{Al}$ . The present calculation assumed the  $0\hbar\omega$  configuration for the ground state of  $^{33}\text{Mg}$ , with  $J^\pi = 7/2^-$ , and used the  $sd$ - $pf$  Hamiltonian from [3]. A  $\beta$ -decay half-life of 77 ms is predicted. Nummela *et al.* report an inversion of the  $\nu(f_{7/2})$  and  $\nu(d_{3/2})$  orbitals in the  $^{33}\text{Mg}$  ground state based on a tentative spin/parity assignment of  $3/2^+$  [22]. This result, from study of the  $\beta$  decay of  $^{33}\text{Na}$ , is inconsistent with the configuration used for the current calculation. More details of the experimental decay scheme and more complete shell model calculations are required for an understanding of the  $^{33}\text{Mg}$  structure.

The continuing improvement of experimental facilities promises to extend the range of  $\beta$ -emitting nuclei available for study. We have used the National Superconducting Cyclotron Laboratory's new Coupled Cyclotron Facility to investigate the  $\beta$  decay of  $^{33}\text{Al}$  and  $^{33}\text{Mg}$ . A precise determination of the  $\beta$ -decay half-life of  $^{33}\text{Al}$ ,  $41.7 \pm 0.2$  ms, has been made. A half-life of  $90.5 \pm 1.6$  ms has been deduced for the  $\beta$  decay of  $^{33}\text{Mg}$ , in agreement with, and considerably more precise than, previous measurements. A  $\gamma$ -ray spectrum from the decay of  $^{33}\text{Al}$  has been obtained and absolute intensities reported for several transitions.

Unlike  $^{32}\text{Mg}$ ,  $^{33}\text{Al}$ , in its ground state, has been shown to be well-described by a shell model calculation made in the  $sd$  shell, suggesting that it lies mainly outside the island of inversion near the  $N = 20$  shell closure.

## Acknowledgements

This work was supported in part by the National Science Foundation, Grants PHY-95-28844, PHY-01-10253 and PHY-00-70911. The authors wish to thank the operations staff at the NSCL for their assistance during this experiment. We also thank J.A. Winger of Mississippi State University and P.L. Reeder of Pacific Northwest National Laboratory for providing unpublished  $^{33}\text{Al}$  results for comparison.

## References

- [1] C. Thibault, R. Klapisch, C. Rigaud, A. M. Poskanzer, R. Prieels, L. Lessard, W. Reisdorf, Phys. Rev. C 12 (1975) 644.
- [2] B. H. Wildenthal, W. Chung, Phys. Rev. C 22 (1980) 2260.
- [3] E. K. Warburton, J. A. Becker, B. A. Brown, Phys. Rev. C 41 (1990) 1147.
- [4] T. Otsuka, N. Fukunishi, Phys. Rep. 264 (1996) 297.
- [5] C. Détraz, D. Guillemaud, G. Huber, R. Klapisch, M. Langevin, F. Naulin, C. Thibault, L. C. Carraz, F. Touchard, Phys. Rev. C 19 (1979) 164.
- [6] T. Motobayashi, Y. Ikeda, Y. Ando, K. Ieki, M. Inoue, N. Iwasa, T. Kikuchi, M. Kurokawa, S. Moriya, S. Ogawa, H. Murakami, S. Shimoura, Y. Yanagisawa, T. Nakamura, Y. Watanabe, M. Ishihara, T. Teranishi, H. Okuno, R. F. Casten, Phys. Lett. B 346 (1995) 9.
- [7] B. V. Pritychenko, T. Glasmacher, P. D. Cottle, M. Fauerbach, R. W. Ibbotson, K. W. Kemper, V. Maddalena, A. Navin, R. Ronningen, A. Sakharuk, H. Scheit, V. G. Zelevinsky, Phys. Lett. B 461 (1999) 322.
- [8] L. K. Fifield, C. L. Woods, R. A. Bark, P. V. Drumm, M. A. C. Hotchkis, Nucl. Phys. A 440 (1985) 531.
- [9] P. Baumann, A. Huck, G. Klotz, A. Knipper, G. Walter, G. Marguier, H. L. Ravn, C. Richard-Serre, A. Poves, J. Retamosa, Phys. Lett. B 228 (1989) 458.
- [10] R. W. Ibbotson, T. Glasmacher, B. A. Brown, L. Chen, M. J. Chromik, P. D. Cottle, M. Fauerbach, K. W. Kemper, D. J. Morrissey, H. Scheit, M. Thoennessen, Phys. Rev. Lett. 80 (1998) 2081.

- [11] J. I. Prisciandaro, A. C. Morton, P. F. Mantica, Nucl. Instrum. and Meth. in Phys. Res. A (in press).
- [12] K. S. Krane, Introductory Nuclear Physics, John Wiley & Sons, New York, 1988.
- [13] D. R. Goosman, C. N. Davids, D. E. Alburger, Phys. Rev. C 8 (1973) 1324.
- [14] W. T. Milner, Oak Ridge National Laboratory, unpublished.
- [15] R. B. Firestone, Table of Isotopes, 8th Edition, Vol. 1, John Wiley & Sons, New York, 1996.
- [16] P. L. Reeder, private communication (2002).
- [17] J. Enders, A. Bauer, D. Bazin, A. Bonaccorso, B. A. Brown, T. Glasmacher, P. G. Hansen, V. Maddalena, K. L. Miller, A. Navin, B. M. Sherrill, J. A. Tostevin, Phys. Rev. C 65 (2001) 034318.
- [18] B. V. Pritychenko, T. Glasmacher, B. A. Brown, P. D. Cottle, R. W. Ibbotson, K. W. Kemper, H. Scheit, Phys. Rev. C 62 (2000) 051601.
- [19] M. Langevin, C. Détraz, D. Guillemaud-Mueller, A. C. Mueller, C. Thibault, F. Touchard, M. Epherre, Nucl. Phys. A 414 (1984) 151.
- [20] B. A. Brown, B. H. Wildenthal, Ann. Rev. of Nucl. Part. Sci. 38 (1988) 29.
- [21] B. H. Wildenthal, M. S. Curtin, B. A. Brown, Phys. Rev. C 28 (1983) 1343.
- [22] S. Nummela, F. Nowacki, P. Baumann, E. Caurier, J. Cederkäll, S. Courtin, P. Dessagne, A. Jokinen, A. Knipper, G. L. Scornet, L. G. Lyapin, C. Miehé, M. Oinonen, E. Poirier, Z. Radivojevic, M. Ramdhane, W. H. Trzaska, G. Walter, J. Äystö, the ISOLDE Collaboration, Phys. Rev. C 64 (2001) 054313.